Reversible magnetization of a $Nd_{1.85}Ce_{0.15}CuO_{4-\delta}$ single crystal

A. A. Nugroho and I. M. Sutjahja
Van der Waals–Zeeman Instituut, Universiteit van Amsterdam, Valckenierstraat 65, 1018 XE, Amsterdam, The Netherlands and Jurusan Fisika, Institut Teknologi Bandung, Jl Ganesha 10, Bandung 40132, Indonesia

A. Rusydi and M. O. Tjia
Jurusan Fisika, Institut Teknologi Bandung, Jl Ganesha 10, Bandung 40132, Indonesia

A. A. Menovsky, F. R. de Boer, and J. J. M. Franse
Van der Waals–Zeeman Instituut, Universiteit van Amsterdam, Valckenierstraat 65, 1018 XE, Amsterdam, The Netherlands

(Received 2 June 1999)

An experimental study has been conducted on the reversible magnetization of a $Nd_{1.85}Ce_{0.15}CuO_{4-\delta}$ single crystal at various magnetic fields applied parallel to the c axis. It was found that the data analyzed following the Hao-Clem model exhibit an excellent fit to the theoretical curve for $H_c(T)$ derived from the BCS model over the relatively broad temperature range from 11.25 K to 19 K (slightly below the critical temperature of 21 K). The result of the analysis yields a constant $\overline{\kappa}$ value of 80 over the temperature range considered. Additional parameters determined in this experiment include $H_{c2}(0)=(9.0\pm0.8)\times10^5$ Oe, $\xi_{ab}(0)=(19.14\pm1.67)$ Å with $\lambda_{ab}(0)=(1493\pm131)$ Å in the dirty limit and $H_{c2}(0)=(6.7\pm0.6)\times10^5$ Oe, $\xi_{ab}(0)=(22.22\pm1.94)$ Å with $\lambda_{ab}(0)=(1733\pm152)$ Å in the clean limit. It is further established from this experiment that the Hao-Clem model is particularly suited for the study of reversible magnetization of low-T_c superconductors with relatively subdued anisotropy such as the sample considered in this study. [S0163-1829(99)02445-5]

The Ginzburg-Landau (G-L) parameter, $\kappa=\lambda/\xi$, is one of the most important characteristics for type-II superconductors both from a fundamental as well as a practical point of view. Before the advent of high-temperature copper-oxide superconductors, this parameter was commonly determined from the magnetization data M according to Abrikosov's formula derived from Ginzburg-Landau theory[1]

$$-4\pi M=\frac{H_{c2}(T)-H}{(2\kappa^2-1)\beta}, \tag{1}$$

which is valid in the vicinity of $H=H_{c2}$. In the case of high-T_c copper-oxide superconductors, most of the available magnetization data are limited to the field region far below H_{c2}, to which Eq. (1) is not applicable. For these high-κ type-II superconductors, the characteristic behavior of the reversible magnetization in the broad intermediate-field region, $H_{c1}\ll H\ll H_{c2}$, was used to be described phenomenologically by the well-known formula derived from the London model,[2]

$$-4\pi M=\frac{\Phi_o}{8\pi\lambda^2}\ln\left(\frac{\eta H_{c2}}{H}\right) \tag{2}$$

exhibiting linear dependence of M on ln(H). This desciption was initially found to agree reasonably well with experimental results.[3–6]

A closer look at the formulation of Eq. (2) by Hao and Clem[7] has revealed, however, a faulty assumption in ignoring the contribution of the core-energy term in the system's free energy density. As a result of inclusion of this additional term, the dimensionless G-L free energy per unit volume over a cross-sectional area A in a plane perpendicular to the vortices becomes[8]

$$F=\frac{1}{A}\int d^2\rho\left[\frac{1}{2}(1-f^2)^2+\frac{1}{\kappa}(\nabla f)^2+f^2\left(\mathbf{a}+\frac{1}{\kappa}\nabla\gamma\right)^2+\mathbf{b}^2\right], \tag{3}$$

where f and γ are the normalized magnitude and phase of the order parameter $\psi=\psi_0 fe^{i\gamma}$, with the vector potential $\mathbf{a}$ and local magnetic flux density $\mathbf{b}$ satisfying the standard relations, $\nabla\cdot\mathbf{a}=\mathbf{0}$ and $\mathbf{b}=\nabla\times\mathbf{a}$. An expression for the reversible magnetization is obtained by means of variational calculation of F using the trial function

$$f=\frac{\rho}{(\rho^2+\xi_\nu^2)^{1/2}}f_\infty, \tag{4}$$

where ρ is the radial coordinate measured from the vortex axis, while ξ_ν and f_∞ are the variational parameters, representing, respectively, the effective core radius of the vortex and the depression of the order parameter due to overlap of the vortices. For the isotropic case, the dimensionless reversible magnetization derived by this method from Eq. (3) is given by[8]

$$\begin{aligned}-4\pi M=&\frac{\kappa f_\infty^2\xi_\nu^2}{2}\left[\frac{1-f_\infty^2}{2}\ln\left(\frac{2}{B\kappa\xi_\nu^2}+1\right)-\frac{1-f_\infty^2}{2+B\kappa\xi_\nu^2}\right.\\&\left.+\frac{f_\infty^2}{(2+B\kappa\xi_\nu^2)^2}\right]+\frac{f_\infty^2(2+3B\kappa\xi_\nu^2)}{2\kappa(2+B\kappa\xi_\nu^2)^3}\\&+\frac{f_\infty}{2\kappa\xi K_1(f_\infty\xi_\nu)}\left[K_0[\xi_\nu(f_\infty^2+2B\kappa)^{1/2}]\right.\\&\left.-\frac{B\kappa\xi_\nu K_1[\xi_\nu(f_\infty^2+2B\kappa)^{1/2}]}{(f_\infty^2+2B\kappa)^{1/2}}\right],\end{aligned} \tag{5}$$

where $K_n(x)$ is a modified Bessel function of nth order. The magnetization M and the magnetic flux density B are related to the thermodynamic magnetic field H by the equation $B = H + 4\pi M$. Confining ourselves to high-κ cases ($\kappa > 10$), one has

$$f_\infty^2 = 1 - \left[\frac{B}{\kappa}\right]^4, \tag{6}$$

$$\left[\frac{\xi_\nu}{\xi_{\nu 0}}\right]^2 = \left[1 - 2\left(1 - \frac{B}{\kappa}\right)^2 \frac{B}{\kappa}\right]\left[1 + \left(\frac{B}{\kappa}\right)^4\right], \tag{7}$$

with $\xi_{\nu 0} = \sqrt{2}/\kappa$.

It was shown in the same reference that the main features of the Abrikosov result can be recovered by this formulation at high field. It was further suggested that an extension of this formula to the anisotropic case can be readily achieved by the introduction of an effective mass tensor or through the simple replacement of κ in Eqs. (5)–(7) by its average value $\bar{\kappa}$. This model has been applied successfully to the analysis of reversible magnetization data of a $YBa_2Cu_3O_7$ single crystal,[8] c-axis-oriented bulk $Bi_2Sr_2Ca_2Cu_3O_8$,[9] c-axis-oriented bulk $YBa_2Cu_4O_8$,[10] polycrystalline bulk sample of $HgBa_2Ca_2Cu_3O_{8-x}$,[11] and polycrystalline bulk sample of $Hg_{0.8}Pb_{0.2}Ba_{1.5}Sr_2Cu_3O_{8-x}$.[12] Instead of its application to high-T_c superconductors, we present in this paper the result of applying this model to the analysis of reversible magnetization data of a low-T_c $Nd_{1.85}Ce_{0.15}CuO_{4-\delta}$ single crystal and the determination of its G-L parameter, κ, as well as the other thermodynamic parameters.

The high-quality single crystal of $Nd_{1.85}Ce_{0.15}CuO_{4-\delta}$ studied in this experiment was grown by the traveling solvent floating zone technique using a four-mirror furnace as reported in a previous paper.[15] As described there, the as-reduced crystal is superconducting at $T_c \sim 21$ K, with a transition width of $\Delta T_c \leqslant 1$ K as determined from its dc susceptibility curve measured by a commercial Quantum Design MPMS-5 magnetometer in a magnetic field of 10 Oe applied parallel to the c axis. The temperature dependence of the magnetization was also measured by the same magnetometer in various magnetic fields ranging between 2500 and 11 250 Oe. The results of these measurements, after substraction of paramagnetic background, are presented in Fig. 1. We note emphatically that these $M(T)$ curves do not exhibit crossover behavior typical for high-T_c copper-oxide superconductors as well as that revealed in the low-T_c $Sm_{1.85}Ce_{0.15}CuO_{4-\delta}$ (SCCO) (Ref. 13) and $Pr_{1.85}Ce_{0.15}CuO_{4-\delta}$ (PCCO).[14] The absence of thermal-fluctuation induced characteristics is apparently related to both the much lower T_c and relatively moderate anisotropy of NCCO compared to other systems mentioned above. It is further noted that each of the magnetization curves in Fig. 1 displays perceptible changes of slope over the entire range of measurement. Consequently, the data must be carefully chosen for their analysis on the basis of the theoretical description given by Eq. (5). In this case, we restrict our M-T data at each field only to those lying in a linear region (satisfying a linear fitting criterion of $R^2 = 0.99$) closest to T_c. These data turn out to be in the temperature range $11.25 \leqslant T \leqslant 19$ K as shown in Fig. 2, and fall into the region of the liquid state in the H-T phase diagram presented in Ref. 15.

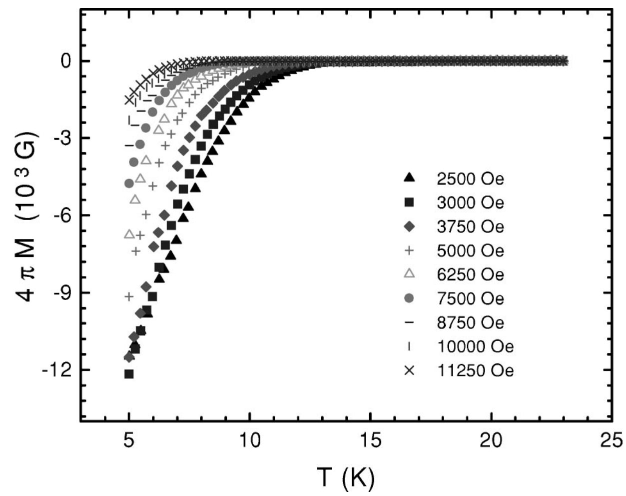

FIG. 1. Temperature dependence of the magnetization in various applied fields between 2500 and 11 250 Oe parallel to the c axis.

The ensuing analysis of these data follows the method and procedure described in Ref. 8. According to this method, the magnetic data M and H at each T should be scaled by $\sqrt{2}H_c(T)$ to yield the normalized data $M' = M/\sqrt{2}H_c(T)$ and $H' = H/\sqrt{2}H_c(T)$ (ignoring demagnetization effect) prior to their analysis. To this end, the data at each T in the range considered ($11.25 \leqslant T \leqslant 19$ K) were sampled in the form of $-4\pi M_i/H_i$ ratios for $i = 1,2,\ldots,$ so that one obtains the required scaled data given by $-4\pi M_i'/H_i' = -4\pi M_i/H_i$. For each of these data corresponding to a certain i, Eq. (5) combined with the relation $H_i' = -4\pi M_i' + B_i'$ and an assumed value of $\bar{\kappa}$ will lead to an equation that can be solved for the corresponding B_i'. From the values of B_i' we further computed the corresponding values of M_i' and subsequently the value of H_{ci} for the particular temperature T considered. The value of H_{ci} generally varies over the whole set of data points ($i = 1,2,\ldots$). However, a systematic search has been carried out for the determination of a $\bar{\kappa}$ value, which produces the set of H_{ci} values with minimum

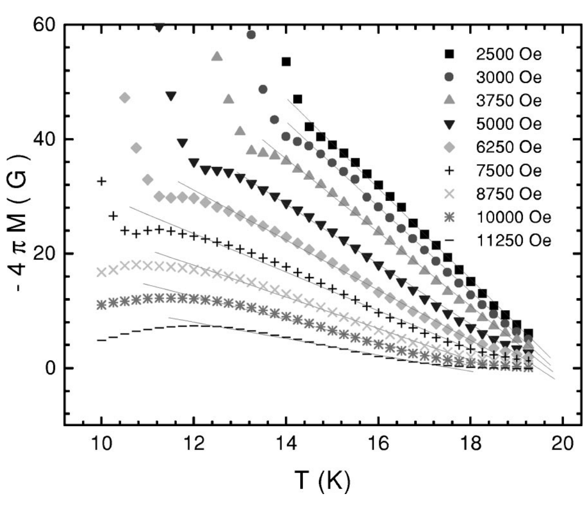

FIG. 2. A close-up view of temperature-dependent magnetization close to T_c extracted from Fig. 1 for various fields. The solid lines are linear fits to the data, which will be used for further analysis.

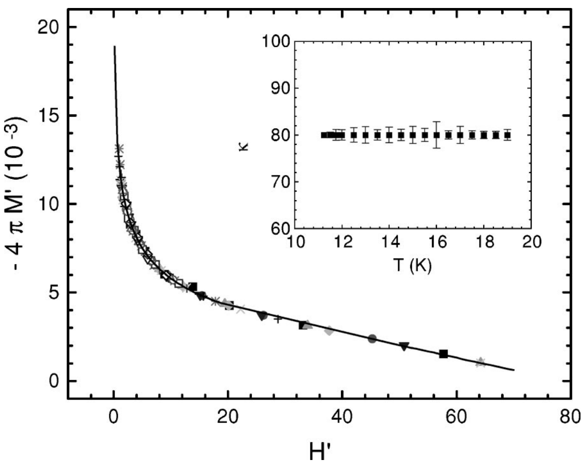

FIG. 3. Scaling of magnetization and applied field with respect to $\sqrt{2}\ H_c(T)$, with the solid curve representing the Hao-Clem model fit for $\bar{\kappa}=80$ for the temperature range from 11.25 to 19 K. The error bars on the curve in the inset indicate the standard deviations of the corresponding average values of $\bar{\kappa}$.

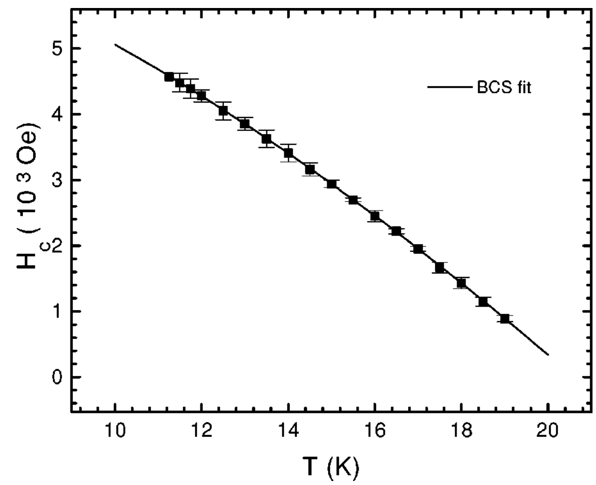

FIG. 4. Temperature dependence of $H_c(T)$ obtained from the result of fitting, and the solid curve represents the theoretical BCS fit with the model for $T_c=20.6$ K. Error bars on the curve indicate the standard deviates of the corresponding average values of $H_c(T)$.

deviation. This procedure is then repeated for each T in the temperature range considered, yielding the corresponding values of M', H', and $\bar{\kappa}$. The result of this analysis is depicted by the $-4\pi M'$ vs H' curve in Fig. 3 and the $\bar{\kappa}$ vs T curve in its inset. It is clear that all the calculated $(-4\pi M', H')$ data are nicely represented by the theoretical curve in the entire temperature range mentioned above, in agreement with the result reported in Refs. 8–12. It is interesting to point out, however, that $\bar{\kappa}$ in the inset remains practically constant over the temperature range considered, in marked contrast to results reported in Refs. 9 and 12, where the drastic departure from mean-field behavior at temperatures close to T_c was observed and attributed to thermal-fluctuation and low dimensionality effects not accounted for by the model proposed in Ref. 8. Being a low-T_c material and having a relatively moderate anisotropy, our sample appears to be particularly suited for the application of this mean-field model.

The result of the fitting described above gives us both the value of $\bar{\kappa}$ and the temperature-dependent function $H_c(T)$ and hence $H_{c2}=\bar{\kappa}\sqrt{2}H_c(T)$. As a further test of our result, the values computed for H_c at each T are plotted with respect to T together with the corresponding standard deviations in Fig. 4. The theoretical curve deduced from the BCS model for $H_c(T)$ is given by[16]

$$\frac{H_c(T)}{H_{co}}=1.7367\left(1-\frac{T}{T_c}\right)\left[1-0.2730\left(1-\frac{T}{T_c}\right)-0.0949\left(1-\frac{T}{T_c}\right)^2\right] \tag{8}$$

and is also plotted in the same figure for comparison. The excellent fit of the calculated data with the theoretical curve shown in the figure is obtained for $H_{co}=(4.80\pm0.5)\times10^3$ Oe and $T_c=20.6\pm1.8$ K, which practically matches the T_c value of 21 K determined separately by dc low-field susceptibility measurement. These near perfect fits in the relatively wide field and temperature ranges in Fig. 3 and Fig. 4 also attest to the appropriateness of our criterion in the choice of data to be analyzed in addition to the validity of the model adopted for the analysis.

The estimation of the coherence length in the ab plane, ξ_{ab}, at zero temperature can be made, assuming isotropy in the plane on the basis of relation, $H_{c2\parallel c}(0)=\phi_0/2\pi\xi_{ab}^2(0)$, while $H_{c2}(0)$ is determined according to the expression[17]

$$H_{c2}(0)=0.5758\left[\frac{\kappa_1(0)}{\kappa}\right]T_c\left[\frac{dH_{c2}}{dT}\right]_{T_c}, \tag{9}$$

where $\kappa_1(0)/\kappa=1.20$ in the dirty limit,[18] and $\kappa_1(0)/\kappa=1.26$ in the clean limit.[19] The slope dH_{c2}/dT can be obtained from Fig. 4 with the help of the relation $H_{c2}(T)\simeq\kappa\sqrt{2}H_c(T)$. The value of this slope at T_c is $(-4.50\pm0.5)\times10^4$ Oe/K. Substituting these values into Eq. (9) yields estimates for the coherence length and the penetration depth, namely, $\xi_{ab}(0)=(19.14\pm1.67)$ Å, $\lambda_{ab}(0)=(1493\pm131)$ Å in the dirty limit and $\xi_{ab}(0)=(22.22\pm1.94)$ Å, $\lambda_{ab}(0)=(1733\pm152)$ Å in the clean limits. It is noteworthy that the values obtained in this study are considerably larger than the values of $\lambda_{ab}(0)\simeq1000$ Å determined by other methods.[20,21] This discrepancy should be a subject of further investigation.

In summary, we have measured the temperature-dependent reversible magnetization of a $Nd_{1.85}Ce_{0.15}CuO_{4-\delta}$ single crystal in various magnetic fields applied parallel to the c axis. The application of the Hao-Clem model to the analysis of these data has shown a consistent fit within the model as well as an excellent fit with the theoretical BCS curve for $H_c(T)$. The result of this analysis yields a constant $\bar{\kappa}$ value of 80 over the temperature range from 11.25 to 19 K, and a slope of $(-4.50\pm0.5)\times10^4$ Oe/K for dH_{c2}/dT at T_c, leading to the values of $H_{c2}(0)=(9.0\pm0.8)\times10^5$ Oe, $\xi_{ab}(0)=(19.14\pm1.67)$ Å, $\lambda_{ab}(0)=(1493\pm131)$ Å for the dirty limit, and $H_{c2}(0)=(6.7\pm0.6)\times10^5$ Oe, $\xi_{ab}(0)=(22.22\pm1.94)$ Å, $\lambda_{ab}(0)=(1733\pm152)$ Å for the clean limit. We further conclude that the near perfect theoretical description as demonstrated in our case, in contrast to previous cases involving high-T_c samples, together with the absence of thermal-fluctuation effects as evidenced by the absence of a crossover in our M-T curves, should clearly suggest the particular applicability of the Hao-Clem model to low-T_c and moderately anisotropic copper-oxide superconductors such as the one studied in this paper. It would be interesting to see if the same quality of fitting could be attained from the data of SCCO and PCCO reported in Refs. 13 and 14, where an unexpected high degree of anisotropy is suggested for the sample.

We thank P. H. Kes for reading the manuscript as well as for comments and suggestions. This work was supported by the Van der Waals–Zeeman Institute through KNAW under Project No. 95-BTM-33 and Jurusan Fisika ITB through RUT project under Contract No. 207/SP/RUT/BPPT/97.

[1] A. A. Abrikosov, Zh. Éksp. Teor. Fiz, **32**, 1442 (1957) [Sov. Phys. JETP **5**, 1174 (1957)].
[2] A. L. Fetter and P. C. Hohenberg, in *Superconductivity*, edited by R. D. Parks (Dekker, New York, 1965), Vol. 1, pp. 138–167.
[3] V. G. Kogan, M. M. Fang, and S. Mitra, Phys. Rev. B **38**, 11 958 (1988).
[4] S. Mitra, J. H. Cho, W. C. Lee, D. C. Johnston, and V. G. Kogan, Phys. Rev. B **40**, 2674 (1989).
[5] J. R. Thompson, D. K. Christen, H. A. Deeds, Y. C. Kim, J. Brynestad, S. T. Sekula, and J. Budai, Phys. Rev. B **41**, 7293 (1990).
[6] M. Tuominen, A. M. Goldman, Y. Z. Chang, and P. Z. Jiang, Phys. Rev. B **42**, 412 (1990).
[7] Z. Hao and J. R. Clem, Phys. Rev. Lett. **67**, 2371 (1991).
[8] Z. Hao, J. R. Clem, M. W. McElfresh, L. Civale, A. P. Malozemoff, and F. Holtzberg, Phys. Rev. B **43**, 2844 (1991).
[9] Qiang Li, M. Suenaga, Junho Gohng, D. K. Finnemore, T. Hikata, and K. Sato, Phys. Rev. B **46**, 3195 (1992).
[10] Junghyun Sok, Ming Xu, Wei Chen, B. J. Suh, J. Gohng, D. K. Finnemore, M. J. Kramer, L. A. Schwatzkopf, and B. Dabrowski, Phys. Rev. B **51**, 6035 (1995).
[11] Mun-Soeg Kim, Myoung-Kwang Bae, W. C. Lee, and Sung-Ik Lee, Phys. Rev. B **51**, 3261 (1995).
[12] Yi Zhuo, Jae-Hyuk Choi, Mun-Seog Kim, Wan-Seon Kim, Z. S. Lim, Sung-Ik Lee, and Sergey Lee, Phys. Rev. B **55**, 12 719 (1997).
[13] L. Fábrega, M. A. Crusellas, J. Fontcuberta, X. Obradors, U. Welp, and G. W. Crabtree, Physica C **194-196**, 2253 (1994).
[14] L. Fábrega, J. Fontcuberta, S. Pinol, X. Obradors, U. Welp, and G. W. Crabtree, Europhys. Lett. **24**, 595 (1993).
[15] A. A. Nugroho, I. M. Sutjahja, M. O. Tjia, A. A. Menovsky, F. R. de Boer, and J. J. M. Franse, Phys. Rev. B **60**, 15 379 (1999).
[16] J. R. Clem, Ann. Phys. (N.Y.) **40**, 268 (1966).
[17] B. Wühlschlegel, Z. Phys. **155**, 584 (1967).
[18] N. R. Werthamer, E. Helfand, and P. C. Hohenberg, Phys. Rev. **147**, 295 (1966).
[19] G. Eilenberger, Phys. Rev. **153**, 584 (1967).
[20] F. Zuo, S. Khizroev, Xiuguang Jiang, J. L. Peng, and R. L. Greene, Phys. Rev. B **49**, 12 326 (1994).
[21] N. C. Yeh, U. Kriplani, W. Jiang, D. S. Reed, D. M. Strayer, J. B. Barner, B. D. Hunt, M. C. Foote, R. P. Vasques, A. Gupta, and A. Kussmaul, Phys. Rev. B **48**, 9861 (1993).